ELSEVIER

International Journal of Heat and Fluid Flow 20 (1999) 477–485

International Journal of HEAT AND FLUID FLOW

www.elsevier.com/locate/ijhff

Experimental investigation of sub-millimetre droplet impingement onto spherical surfaces

Y. Hardalupas *, A.M.K.P. Taylor, J.H. Wilkins

Mechanical Engineering Department, Imperial College of Science, Technology and Medicine, Exhibition Road, London SW7 2BX, UK

Abstract

This study reports an experimental investigation of the phenomena which occur when discrete, monodisperse droplets of a water–ethanol–glycerol solution in the size and velocity ranges of $160 < D < 230$ μm and $6 < U < 13$ m/s, respectively, impinge upon a spherical surface with diameter of the order of 1 mm. By altering the concentrations of the water, ethanol and glycerine, the surface tension and viscosity were varied in the ranges $58 < \sigma < 73$ mN/m and $0.0010 < \mu < 0.0024$ kg/ms, respectively. The boundary between droplets that deposit and droplets that reatomise has been quantified and an empirical correlation in terms of kinematic and liquid properties is reported. The target surface diameter was varied in the range 800–1300 μm and compared with a plane surface of equivalent non dimensional roughness; increasing surface curvature was seen to promote the onset of reatomisation. Stroboscopic images of the impingement process showed that the impinged droplet formed a crown which was influenced by both surface roughness, varied in the range 35 nm–40 μm, and droplet kinematic and liquid properties. The similarity in the trajectories of reatomised droplets produced from consecutive crowns implied that the reatomisation mechanism was repeatable and influenced by surface morphology.

Notation

a	exponent in deposition/splashing boundary equation
D	impinging droplet diameter
K	coefficient identifying deposition/splashing boundary
Oh	Ohnesorge number defined as $\mu/\sqrt{(\rho\sigma D)}$
R_a	surface roughness
Re	Reynolds number defined as $\rho UD/\mu$
U	impinging droplet vertical velocity component
We	Weber number defined as $\rho DU^2/\sigma$
Greek	
δ	target sphere diameter
δ^*	target sphere curvature defined as $1/\delta$
μ	liquid absolute viscosity
ρ	liquid density
σ	liquid surface tension

1. Introduction

The interaction of liquid sprays and their constituent droplets with either liquid or solid surfaces is an area of fluid mechanics with numerous applications and manifestations in both engineering and nature. The present experimental study has investigated the phenomena which occur when discrete monodisperse droplets impinge upon a rigid, spherical surface with curvature of similar order to that of the incident droplet. Such a situation occurs, for example, in fluidised beds and pharmaceutical manufacture when solid particles are brought into contact with liquid droplets within the production plant in order to promote agglomeration, or growth by layering of solids upon the particle. Droplet impingement onto plane surfaces is another situation of practical importance and occurs, for instance, when petrol or diesel fuel is injected onto a piston crown in an IC engine, or during the cleaning of surfaces by high pressure sprays.

After impingement onto a solid surface, this study observed that a droplet generally forms a crown-like structure, the dimensions of which depend upon the surface and impingement conditions: impinging velocity, droplet diameter, liquid properties and surface curvature and roughness. For impinging droplets with significantly lower velocity than those in the present experiments, for instance with U of ~2 m/s, it is reported (Stow and Hadfield, 1981) that there is only a radial flow out of the impinged droplet, with no visible crown formation. However for the droplets employed in the present study, a liquid crown was always observed to form during impingement, leading to reatomisation and reatomised, or secondary, droplet production for sufficiently large U or D, or low μ or σ. Otherwise, all the liquid mass deposited upon the surface, which may be desirable in, for example, the practical application of particle production. Eq. (1) indicates the empirically determined relationship between these parameters which governs the limit between deposition and reatomisation.

Several works have been published concerning impingement onto plane surfaces; the importance of surface roughness R_a, droplet kinematic properties U and D, and

* Corresponding author. E-mail: y.hardalupas@ic.ac.uk

0142-727X/99/$ – see front matter
PII: S0142-727X(99)00045-4

liquid properties of μ, ρ and σ is described in Levin and Hobbs (1971); Stow and Hadfield (1981) and Yarin and Weiss (1995). For the case of spherical surfaces, one can add the target sphere diameter, δ, as a controlling influence. As shown by the energy balance approach of Mundo et al. (1995), these variables can be grouped together into dimensionless groups known as the Reynolds number, Re, and the Ohnesorge number, Oh. Another dimensionless group that is commonly used in the study of atomisation and reatomisation is the Weber number, We. The Weber number represents the ratio of dynamic pressure to surface tension forces and the Reynolds number represents the ratio of inertial forces to viscous forces. The relationship between the three dimensionless groups is such that $\mathrm{Oh} = \sqrt{\mathrm{We}}/\mathrm{Re}$. Throughout the remainder of this paper, the Ohnesorge and Reynolds numbers, and not the Weber number, are the dimensionless groups which are chosen to be used. For plane surfaces, the boundary dividing deposition from reatomisation can be empirically described (Mundo et al., 1995), (Stow and Hadfield, 1981) in the form

$$K = \mathrm{Oh}\ \mathrm{Re}^a, \tag{1}$$

where a was found experimentally (Mundo et al., 1995) to be 1.25 and K is constant for a given surface and is dependent upon its roughness. A similar empirical equation representing this boundary for curved surfaces has been determined in the present study and is reported in Section 3.3.

For impingement conditions which do lead to reatomisation, it is important to visualise the mechanism by which the smaller, reatomised droplets are produced. The behaviour of reatomised droplets is of practical interest. For the example case of particle production, the liquid contained within these small droplets may evaporate on the heated air stream in the plant to produce tiny solid 'fines' which can be entrained upon the bulk air flow within the plant and exhausted to the environment unless expensive steps are taken to filter them at the exhaust. To qualitatively see how the reatomised droplet sizes are affected by impingement conditions of U, D, δ and R_a, this study has visualised, with an imaging system based around a CCD camera, the reatomisation mechanism that acts upon a crown. Selected images showing characteristic features of the reatomisation process, together with proposed explanations of the phenomena which occur in each image, are presented in Section 3.2. To understand at what times during the impingement process the reatomised droplets are produced, and what velocity vector they might be expected to have, temporal developments of the velocity of the characteristic crown geometrical features of crown base and crown rim have been made and are reported in Section 3.1. These were obtained from a montage of stroboscopic CCD camera images, each taken from a separate droplet to give a synthesised history of the impingement event. Similar photographic records of the impingement of larger, millimetre sized droplets onto dry plane surfaces can be found in Stow and Hadfield (1981). Investigations which have used Phase Doppler Anemometry (PDA) to quantify the reatomised droplet sizes from impingement of sub-millimetre monodisperse droplets include Mundo et al. (1995), who used a dry surface, and Ghielmetti et al. (1997), who used a surface covered with a thin film. For a dry surface, Mundo et al. (1995) found the reatomised droplet sizes had an arithmetic mean diameter of around 0.15 that of the impinging droplet. However it appears, Ghielmetti et al. (1997), that a film upon the surface can produce reatomised droplets with an arithmetic mean of around 0.4 times that of the impinging droplet, and a fraction of reatomised droplets with a diameter approaching that of the impinging droplet. This indicates that entrainment of the liquid film upon the surface can significantly increase reatomised droplet size.

The repeatability of the present reatomisation mechanism is expected to be considerably higher than that which can be measured at the exit of a typical pressure atomiser. A repeatable reatomisation mechanism implies a deterministic influence of the morphology of the surface upon the crown breakup, as opposed to random breakup by aerodynamic instabilities. In Section 3.4, the repeatability of the reatomisation mechanism has been quantified on the basis of similarity in the Cartesian locations of the reatomised droplets produced from consecutive impingements.

2. Experimental arrangement and instrumentation

The test rig is shown schematically in Fig. 1. Monodisperse droplets were produced by a custom made monodisperse droplet generator. Liquid was supplied to the droplet generator from a 5 l reservoir pressurised by a regulated air supply, typically at 80–150 kPa gauge pressure. It is then issued through a 100 μm diameter orifice fastened onto the end of the droplet generator body to form a laminar jet. The droplet generator body was fixed between two piezoelectric transducers which, when excited by an a.c. voltage from a signal generator, produced a dilational wave upon the jet. For frequencies which were inherently unstable, the jet broke up through the *Rayleigh* (McCarthy and Molloy, 1974) mechanism to produce a stream of monodisperse droplets, the size of which could be controlled, when using a 100 μm orifice diameter, to be in the range of $160 < D < 230$ μm. The upper and lower bounds of these excitation frequencies were 10 and 32 kHz, respectively. Test solutions of water–ethanol–glycerine combinations were used to vary liquid properties of surface tension and viscosity in the ranges $58 < \sigma < 73$ mN/m and $0.0010 < \mu < 0.0024$ kg/ms. The measurements of viscosity were made with a Ostwald viscometer and those of surface tension with an electronic tensometer. To ensure discrete impingements uninfluenced by adjacent droplets, an electrostatic deflector system was built to charge, with charging electrodes operating at around 50 V, typically 95% of the droplet stream as the droplets broke off from the earthed jet issuing from the earthed body of the monodisperse droplet generator. These charging electrodes were periodically discharged every 19th droplet produced by the monodisperse droplet generator, for a time equal to around 75% of the period of the a.c. piezo electric transducer excitation signal, to produce 5% of the droplets without charge. Synchronisation between droplet generator and charging electrodes was achieved by controlling them both from a master timer card inside a computer. Approximately 20 mm downstream of the charging electrodes were two parallel deflector electrodes; one at around −1.5 kV and the other at earth potential. The electric field between the two deflector electrodes deflected the charged portion of the droplet stream laterally by around 3 mm into a drain leaving only the uncharged 5% to continue downwards and impinge upon the test surface. Consequently the temporal interdroplet spacing of the undeflected droplets, which were then able to impinge on the test surface, was typically 1 ms. By both altering the pressure of the air supply in the range 80–150 kPa and adjusting the height of the droplet generator above the impinging target in the range 30–200 mm, it was possible to vary the impinging velocity between $6 < U < 13$ m/s. The target sphere upon which the droplets impinged was made from stainless steel of $R_a \sim 35$ nm. Different spheres of diameter, δ, 800, 1020 and 1300 μm were used to investigate the effect of surface curvature. The target sphere could be positioned with a micrometer driven device directly under the impinging droplets. The measuring volume of a 30 mW He–Ne laser and Phase Doppler Anemometer (PDA) system was situated

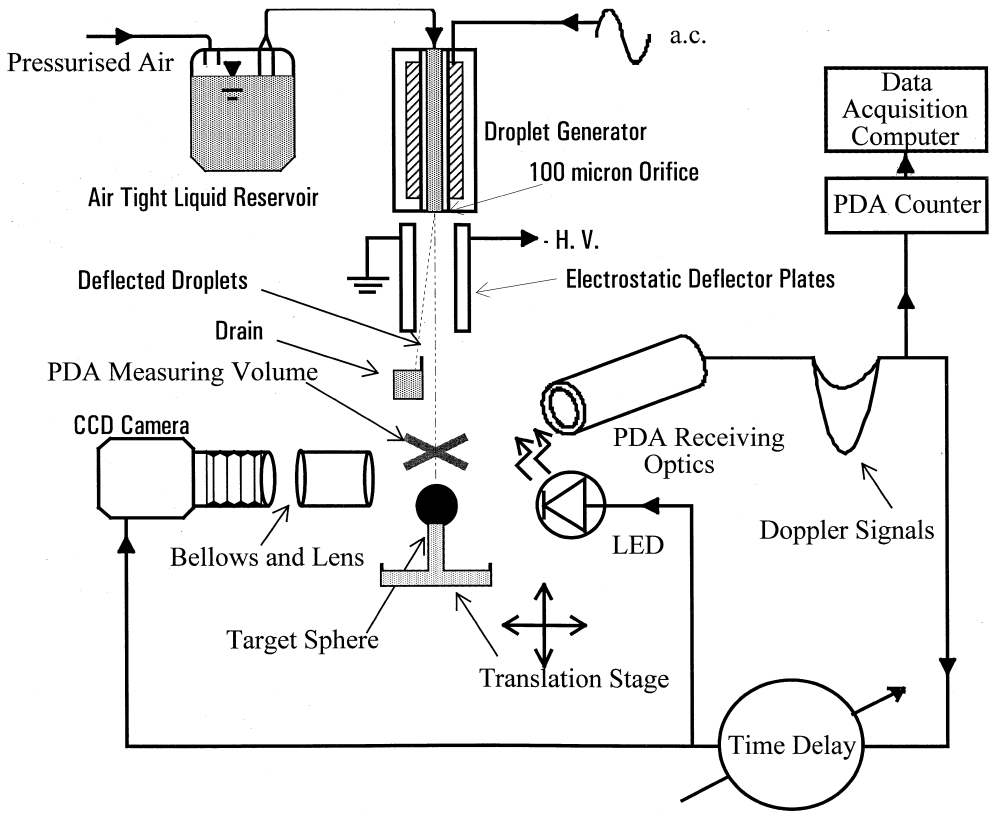

Fig. 1. Schematic of the test rig and associated instrumentation.

≈1 mm above the target sphere. The resulting Doppler burst not only gave information on the velocity and diameter of the impinging droplet via the PDA signal processor, but was also used to trigger an intensified CCD camera and high intensity LED illuminator, capable of producing temporal image, or 'shutter', widths of 500 ns, so 'freezing' the details of the impingement process. By introducing variable time delays of up to 150 μs into the triggering circuit, stroboscopic images at different stages of the impingement process were obtained, enabling a synthesised history to be constructed.

There was sufficient time, typically 1 ms, between successive impingements to allow most of the liquid deposited on the target sphere to drain away under the influence of gravity. Despite this, a thin film inevitably remained upon the surface but with thickness of only ≈2.5% of the impinging droplet diameter. This was measured from CCD images of how the apparent diameter of the sphere changed from the value observed immediately at the end of an impingement to that 1 h after the experiment was stopped and the residual film had drained and evaporated away. The effect of thin film thickness upon droplet impingement phenomena onto plane surfaces was investigated by Cossali et al. (1997) who report that the result of similarly small thickness is to increase K by only ≈1%.

3. Results and discussion

3.1. Formation and propagation of droplet crown

Fig. 2 shows a selection of typical images of crowns that formed during the impingement processes reported within this study; in all cases the test liquid was water but the velocities and diameters of the droplets and the surface conditions have been varied to illustrate a variety of phenomena which can occur. Fig. 2a illustrates the early development of a crown 5 μs after initial impingement of a droplet. Immediately after initial contact between the apex of the droplet and the sphere, the downward motion of the droplet trapped and compressed a segment of liquid between the unyielding sphere and the contact edge of the droplet (Bowden and Field, 1964). This segment contained an envelope of shock wavelets, each wavelet having been generated at a point along the circumference of the droplet as it meets the solid surface. At first, the tangent to the droplet circumference at the contact edge with the solid surface was sufficiently horizontal that, in a small time increment δt, the contact edge could move an adequate distance vertically downward in front of the expanding shock envelope so as to continue trap the compressed liquid inside the droplet. However as time increased and the droplet translated down over the surface of the sphere, this tangent became progressively orientated towards the vertical from the initial horizontal angle of 0°. There was a critical time after initial impingement when the contact edge could not move sufficient distance downwards to continue to be in front of the envelope of shock waves. Consequently, the compressed liquid segment could then overtake the contact edge and cause release of the high pressure liquid in the form of jetting at supersonic velocity. The time at which this release occurred is a function of U, (Bowden and Field, 1964), and can be estimated for the present case to be of the order of nanoseconds. This is orders of magnitude smaller than the timescales upon which the crown can be seen to have developed macroscopically in Fig. 2.

The crown developed in the first 10 μs with characteristic velocities several times higher than U. This is evident in Fig. 3, which shows the temporal development of the velocity of the crown base in the radial direction, the crown base in the vertical direction, and the crown rim relative to the base in the vertical direction. The data for these plots came from

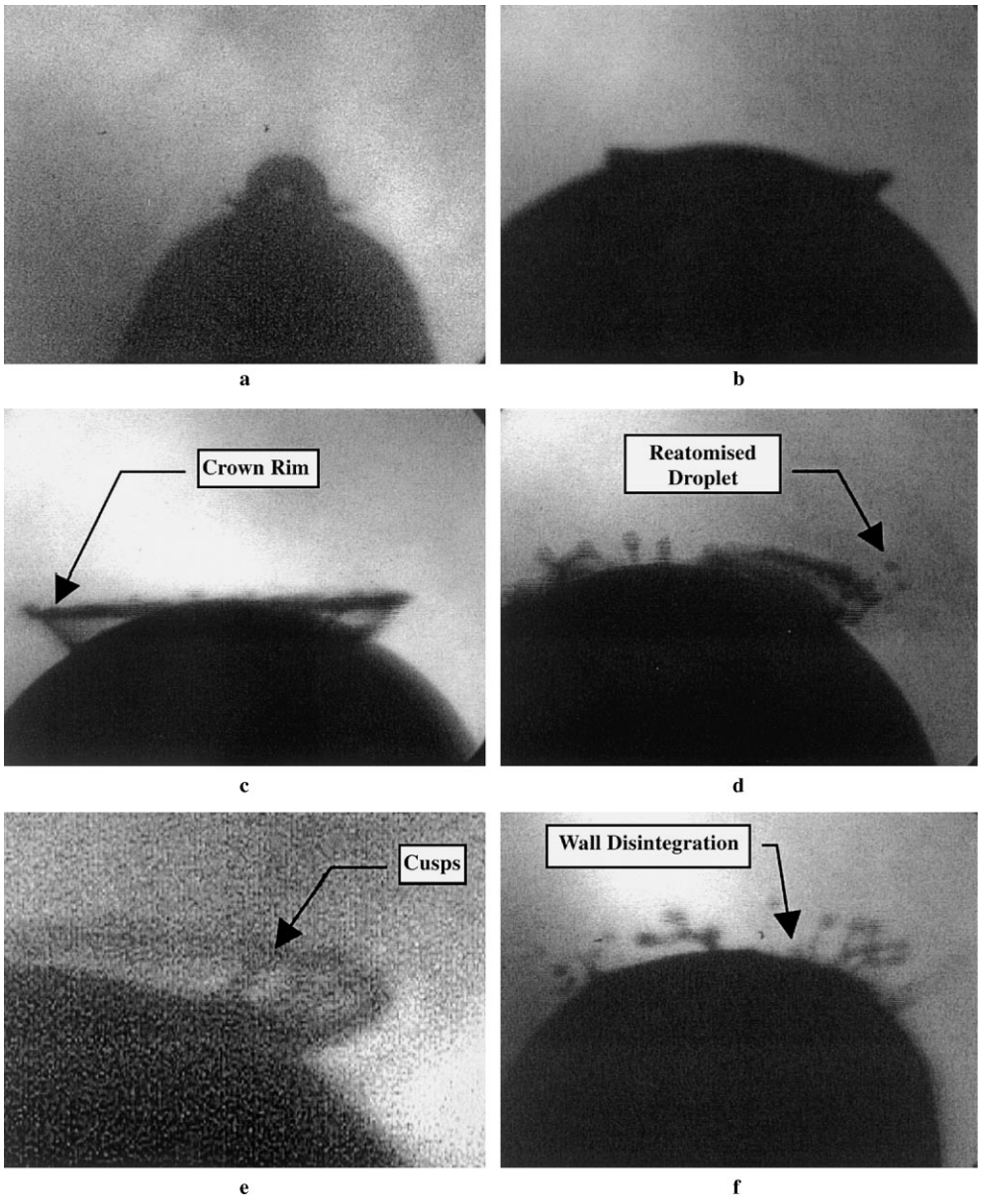

Fig. 2. Characteristic images of droplet impingement phenomena. Taken with water as the test liquid and with a 500 ns image 'shutter speed'. The impinging velocity and diameter, surface diameter and condition and time after initial impingement of each image is given. (a) Crown Formation. $D = 220$ μm, $U = 10.8$ m/s, $\delta = 800$ μm , $R_a = 35$ nm, 5 μs. The scale of the image is 5.5 mm (upon the image) : 100 μm (in the experiment). (b) Low Momentum Crown. $D = 184$ μm, $U = 7.5$m/s, $\delta = 1300$ μm, $R_a = 35$ nm, 45 μs. The scale is 7 mm : 100 μm. (c) Higher Momentum Crown. $D = 218$ μm, $U = 9.5$m/s, $\delta = 1300$ μm, $R_a = 35$ nm. 45 μs. The scale is 6.75 mm : 100 μm. (d) Crown Breakup and Finger Formation. $D = 221$ μm, $U = 9.5$m/s, $\delta = 1300$ μm, $R_a = 35$ nm, 55 μs. The scale is 7.25 mm : 100 μm. (e) Cusps Upon Crown. $D = 220$ μm, $U = 9.3$ m/s, $\delta = 800$ μm, $R_a = 35$ nm, 20 μs. The scale is 11 mm : 100 μm. (f) Rough Surface. $D = 222$ μm, $U = 9.3$ m/s, $\delta = 1300$ μm artificially roughened with 20 μm asperities. 60 μs. The scale is 5.25 mm: 100 μm.

calibrated measurements from a montage of images taken of the crown formed from impingement of droplets with D of 220 μm and impingement U of 10.8 m/s onto a nominally smooth, $R_a = 35$ nm, sphere with δ of 1300 μm. Additionally, the law described in Yarin and Weiss (1995) which specifies the radial displacement of an inviscid crown base as proportional to the square root of time after initial impingement has been differentiated with respect to time and then plotted in Fig. 3 to determine how well it applies to the impingement onto spherical surface of δ of 1300 μm. The coefficient of proportionality used in Fig. 3 has been chosen empirically to give the best correspondence with the plotted experimental data. One can see how the radial velocity of the crown base quickly decreased in the first 10 μs, due to a combination of the retardation effect of the liquid viscosity, conservation of radial momentum, and the increasing orientation of the tangent to the contact edge towards the vertical so changing the direction of the velocity vector of the crown base. After 35–40 μs from initial impingement, the crown rim velocity relative to the base became negative, indicating the onset of collapse of the crown. The influence of gravity upon the crown can be estimated to have been small, implying that the cause of the collapse was due to surface tension driven recoil of the rim of the crown and conservation of mass, given that the crown was continually

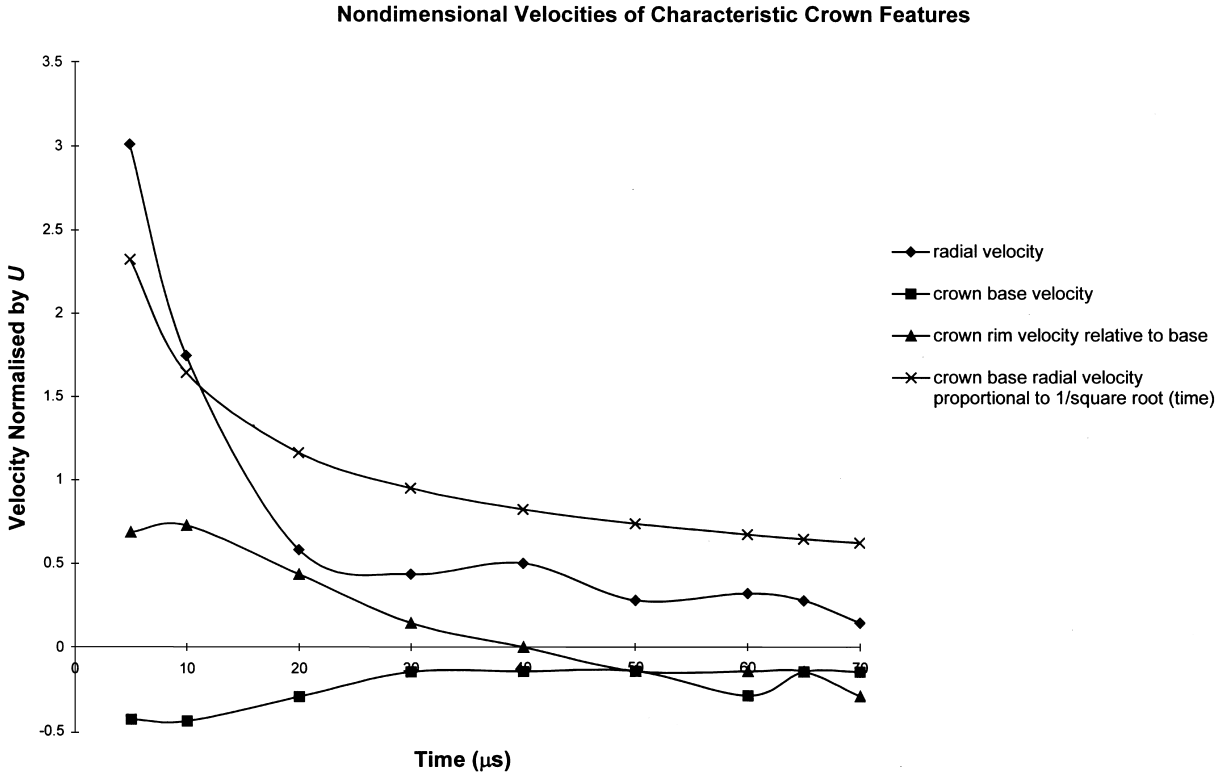

Fig. 3. Nondimensional characteristic crown velocities as a function of time after initial impingement of a water droplet with $D = 220$ μm, $U = 10.8$ m/s, $\delta = 1300$ μm, $R_a = 35$ nm.

expanding in the radial direction. Notice that the absolute vertical velocity of the crown rim was, after 35–40 μs, in a downwards direction, i.e., in the same direction as the parent droplet and the force of gravity. The majority of reatomised droplets were seen to leave the crown after around 50 μs from initial impingement. Since the reatomised droplets were produce at the rim of the crown, the vertical component of the velocity of these droplets was also directed downwards. Fig. 3 implies that the absolute vertical component of their velocity at this time was approximately 0.25 U. Additional measurements with a PDA instrument, not reported in this paper, confirmed this value. This is in contrast to the results of Mundo et al. (1995), where the vertical velocity component of the reatomised droplets was reported to be upwards from the plane test surface, in a direction opposite to the force of gravity. The theoretical relationship, derived from Yarin and Weiss (1995), for the crown base radial velocity as being inversely proportional to square root of time after initial impingement can be seen to overestimate the radial velocity, particularly at the later times during the impingement process. This is presumably due to a combination of the neglection of viscous effects in the theory and the curvature of the surface, which directed the motion of the base of the crown towards the vertical direction, particularly at later times during the impingement process when the local surface slope experienced by the base of the crown became less orientated towards the horizontal than its initial value at the apex of the sphere.

3.2. Effect of impingement conditions upon the crown

Fig. 2b and c illustrate the effect of impinging droplet momentum on crown development. The former case is seen to have resulted in benign deposition with a relatively low, thick crown whereas the latter higher momentum impingement produced a tall, thin crown which took significantly longer to decay: 70 μs as opposed to 50 μs. The influence of surface tension upon the upper edge of a crown produces a rim thicker than the wall of the bulk of the crown. If the constant K, Eq. (1), of the impinging droplet is sufficiently large, the resulting crown can be thin enough and have sufficient velocity for instabilities to grow and cause cusps, such as those shown in Fig. 2e, which appear as swallowings of the crown wall. As the cusp amplitude increases, the rim on either side of a cusp can touch together and merge and can be seen to result in finger-like structures propagating outwards, Fig. 2d. A description of how these fingers can be disrupted through the mechanism of *Rayleigh* breakup (McCarthy and Molloy, 1974) to undergo reatomisation and produce reatomised droplets is given by Yarin and Weiss (1995). It was observed that the typical times at which reatomised droplets were produced was around 50–70 μs after initial impingement, and that after a time of 40 μs, crown collapse started to occur, as indicated on Fig. 3. Thus, it is proposed that crown collapse has a destabilising effect upon a crown and its cusps, promoting the rim merger and finger-like structure generation that are necessary for reatomisation to occur.

The surface roughness of the target sphere was varied deliberately and was seen by observation with the CCD camera to influence both the crown formation process and the nature of its subsequent breakup. Asperities promote the disturbances on a crown which grow to cause cusp formation, and in severe cases can lead to disintegration of the wall beneath the rim consisting of the bulk of the crown. Fig. 2f shows a sphere that was artificially roughened by adding 20 μm diameter glass beads on the surface. As well as reatomisation via the aforementioned Rayleigh instability breakup mechanism, large-scale destruction of the crown was observed, which produced a greater flux of reatomised liquid and wider range of sizes of

reatomised droplets than for a smooth surface. The time at which the crown began to break up on the roughened surfaces was around 20–30 μs after initial impingement. This is sooner than the corresponding time for a smooth surface.

3.3. Boundary between deposition and reatomisation

As Fig. 2b and c show, it is possible to classify an impingement event as either leading to benign deposition, or to reatomisation and formation of reatomised droplets. It is important to quantify the boundary between the two regimes in terms of droplet kinematic and liquid properties. For droplets with properties in the ranges $160 < D < 230$ μm, $58 < \sigma < 73$ mN/m, and $0.0010 < \mu < 0.0024$ kg/ms, the velocity of impingement was altered to get pairs of conditions which could be seen, by visual observation with the imaging system, to straddle the boundary. These conditions are plotted in Fig. 4 in terms of the Re and Oh numbers of the impinging droplets, which were varied in the ranges $800 < \mathrm{Re} < 1750$ and $0.008 < \mathrm{Oh} < 0.020$, respectively. The uncertainties in the Re and Oh numbers are expected to have been around 1.6% and 1.5%, respectively. Results are presented for smooth spherical target surfaces of $R_a \sim 35$ nm and δ of 800 and 1300 μm, and for two artificially roughened spherical targets of δ of 1300 μm and mean asperity height 20 and 40 μm, respectively. For comparison with plane surfaces, the results of Mundo et al. (1995) have been included in Fig. 4, having first been modified for the effect of differing surface roughness between the two experiments, in accordance with Cossali et al. (1997), to give the coefficients in Eq. (1) as $K = 90$ and $a = 1.25$. The effect of increasing target sphere curvature is seen to promote splashing; for the smooth target sphere of δ of 1300 μm, $K = 69$ and $a = 1.22$ whilst for δ of 800 μm, $K = 48$ and $a = 1.18$. The uncertainties in Re and Oh are estimated to have led to an uncertainty in K of 2.5%. One may illustrate the values of these dimensionless numbers in terms of the critical U required for the onset of reatomisation for a water droplet of D of 200 μm; the critical U for a plane surface (Mundo et al., 1995) is 8.3 m/s, whilst for the smooth target sphere with δ of 800 μm it is lower at 7.6 m/s. To further illustrate the observation that increasing target sphere curvature promotes splashing, an additional, intermediate set of measurements for δ of 1020 μm are included in Fig. 5, which shows how K varies with surface curvature, δ^*. A parabolic curve fit, albeit based tentatively on only four data points, has been superimposed and is seen to fit well the available data within the range $0 < \delta^* < 0.00125$ μm^{-1}. If one assumes an overall value for a valid for all the target spheres that is the mean of $a = 1.18$ and $a = 1.22$, then the relationship between deposition and splashing on curved surfaces can be expressed in the form

$$K = g(\delta^*)\mathrm{Oh}\,\mathrm{Re}^a, \tag{2}$$

where $g(\delta^*)$ is the parabolic function of Fig. 5 and has been found empirically to be

$$g(\delta^*) = 90 - 30 \times 10^6(\delta^*)^2. \tag{3}$$

In Mundo et al. (1995) the form of the reatomisation boundary for a plane surface was theoretically predicted by performing an energy balance on the droplet before and at the end of impingement. It was assumed that the impinged droplet would spread radially over the solid surface, and that if the deposited liquid had a non zero kinetic energy at the maximum radius of spreading, then this energy would be manifested as a crown from which reatomisation was implicitly assumed to occur. For the present case a qualitative estimate, based on a similar approach to Mundo et al. (1995), of the effect of

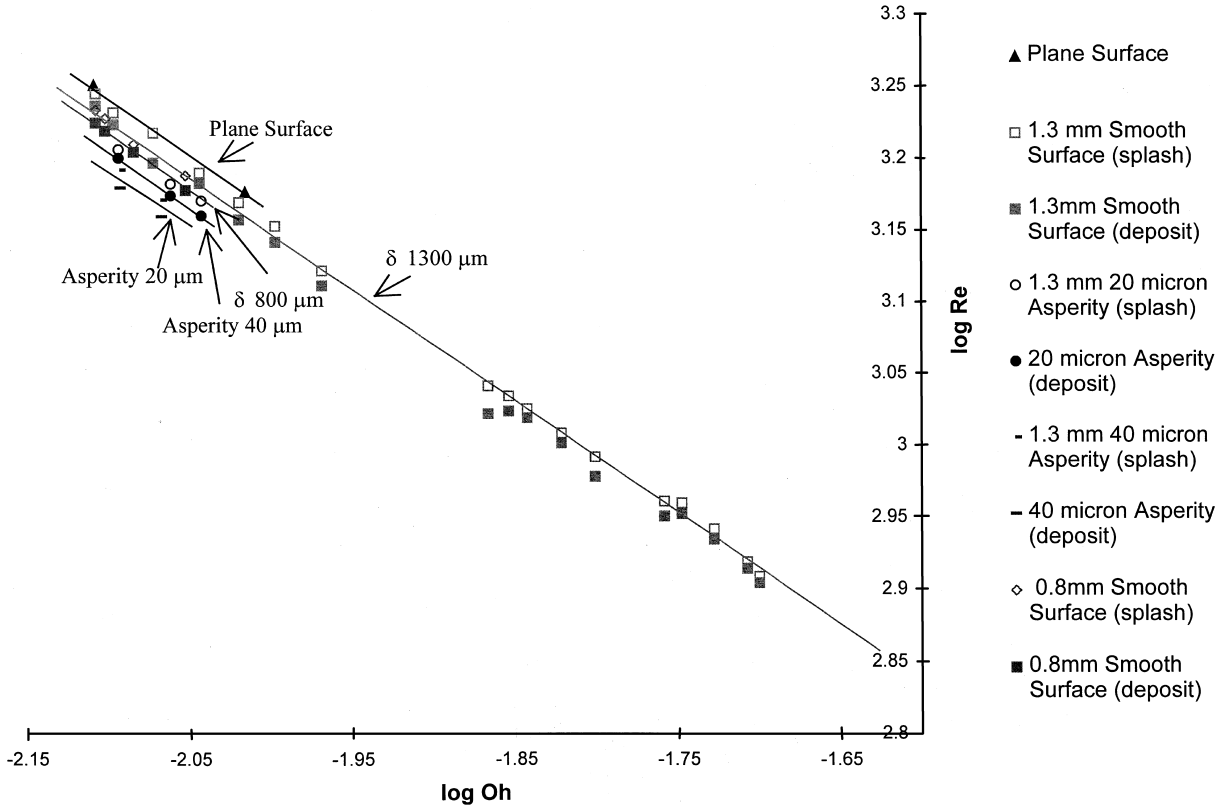

Fig. 4. The boundary between deposition and reatomisation.

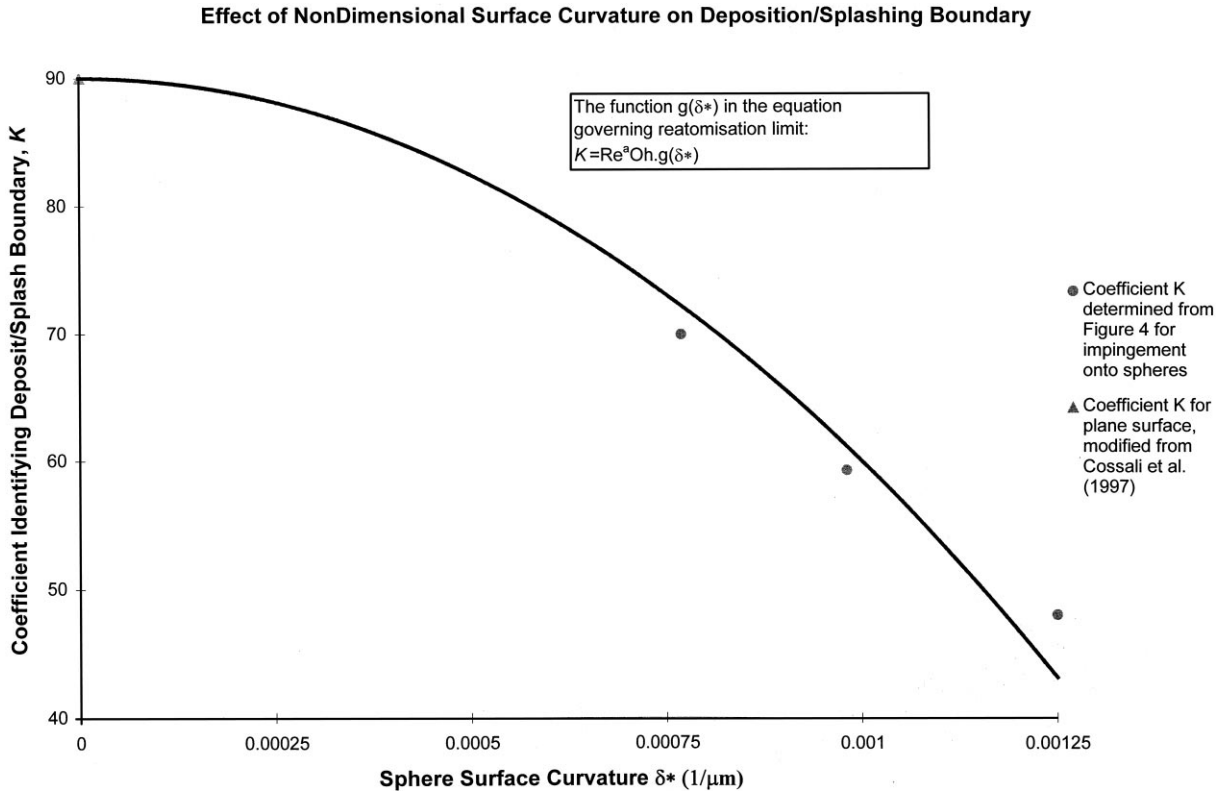

Fig. 5. The variation of parameter K with sphere curvature δ^*.

spherical target curvature on the post impingement energy terms reveals the post radial spreading kinetic energy to be lower, primarily because of greater work done against viscous forces, and greater surface energy of the deposited liquid geometry. This is because the distance travelled over the surface of the sphere by the liquid in the impinged droplet until it reaches its maximum radius of spreading will be greater since the liquid moves not only radially outwards, but also vertically downwards over the sphere. However Fig. 2b shows that in the present series of experiments, even for the deposition regime, a crown formed, albeit sufficiently short and thick that it never formed the disrupting finger-like structures seen in Fig. 2c from which reatomisation occurred. Thus crown formation is seen to be a necessary but not sufficient condition for reatomisation to occur. It appears that an additional important condition for reatomisation is that the cusps upon a crown be allowed to grow in amplitude to allow adjacent sides of the rim to merge and so produce the finger-like structures; as previously discussed this appears to happen when the collapse of the crown destabilises the crown and the cusps. This event is dependent not only on sufficiently high crown height and sufficiently thin crown thickness, but also upon crown diameter. As crown diameter decreases, the acute angle between the two sides of the rim on adjacent sides of a cusp will also decrease, increasing the ease with which the sides can touch together and merge and produce the necessary finger-like structures for reatomisation. Since the motion of the base of the crown follows the surface of the spherical target, decreased target sphere diameter decreases the crown diameter and thus promotes reatomisation.

3.4. Repeatability of the reatomisation process

The repeatability of the reatomisation phenomena in the present experiment was high in comparison to the stochastic breakup behaviour usually exhibited at the exit of pressurised atomiser sprays. Fig. 6 shows the Cartesian co-ordinate location of typical reatomised droplets produced from a small portion of the crowns from 50 separate impingements. Each location was measured from images taken 100 ± 2.5 μs after the arrival of droplets of diameter 221 μm and velocity 9.3 m/s impinging at a rate of 550 Hz. These values of velocity and diameter were chosen to give Re and Oh in the middle of the range of values that could be obtained in the present series of experiments when using water as the test liquid. Due to the relatively slow 25 Hz frame rate of the imaging system, successive images do not represent adjacent impingements, but given the repeatability of the experiment this does not affect the observations. The mean and standard deviation of the locations of the reatomised droplets are: in the horizontal, x, direction, 603 and 18 μm, respectively; and in the vertical, y, direction −325 and 20 μm, respectively. The close grouping of droplet positions suggests a deterministic reatomisation process and thus a laminar flow within the crown. Since the reatomised droplet production resulted from breakup of finger-like structures preceded by cusp formation, one can infer that those features of the crown also exhibited high repeatability. Cusp formation results from growth of initial disturbances upon the crown. Thus, in the spectrum of disturbances to which a crown is exposed, those due to the predictable surface morphology of the target sphere must then dominate those of a purely random aerodynamic and hydrodynamic nature. This implies that computational modelling of the crown requires accurate representation of the surface of the target sphere with resolutions similar to those of the topographical features of the surface.

4. Conclusions

The phenomena occurring when monodisperse droplets of varying Reynolds and Ohnesorge number, in the ranges

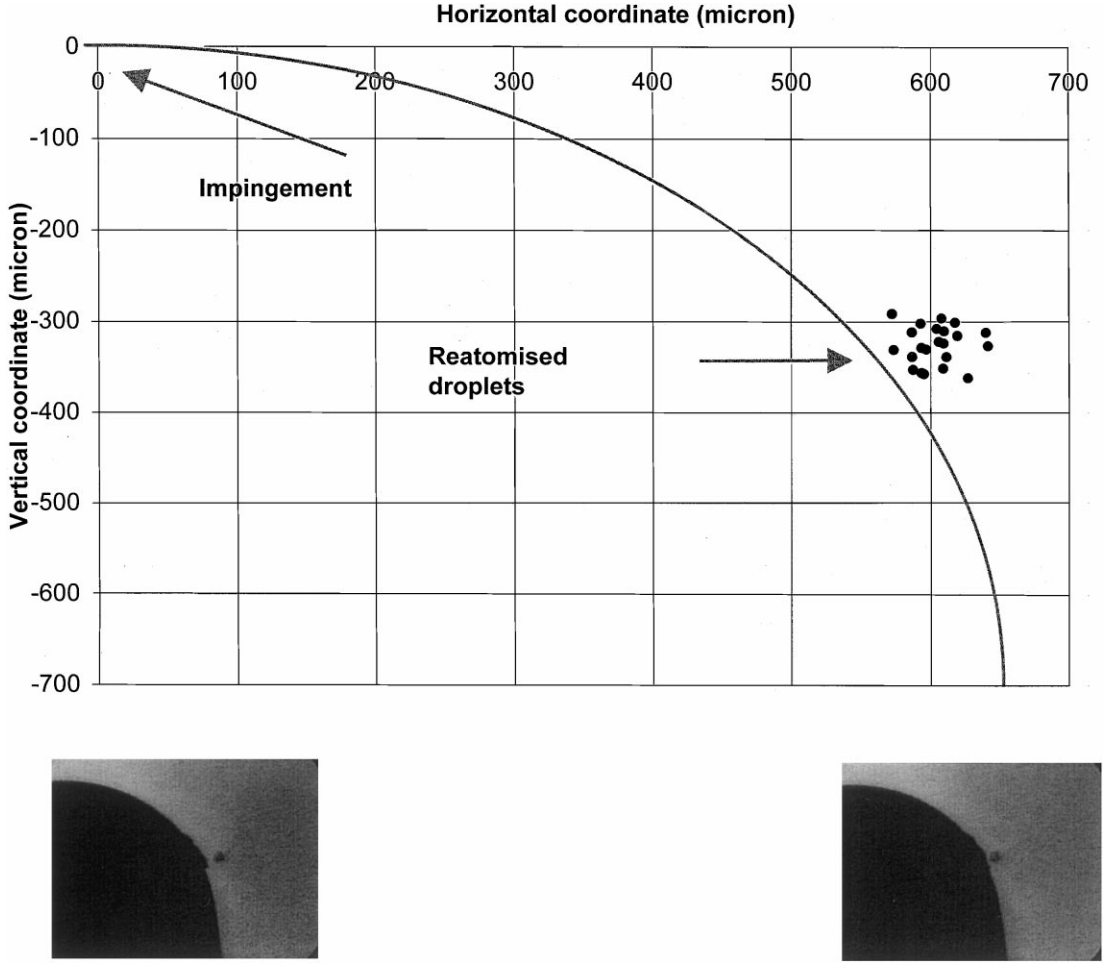

Fig. 6. The repeatability of the reatomisation process. Reatomised droplet positions 100 ms after initial impingement for 50 separate events are shown relative to the outline of the target sphere. Two such images are illustrated below the graph, separated in time by 40 ms.

800–1750 and 0.008–0.020, respectively, impinge upon a spherical target, of diameter in the range 800–1300 μm, have been experimentally investigated. An imaging system based around a CCD camera and triggered by the impinging droplets allowed stroboscopic images at variable times within the impingement process to be obtained. Analysis of these images has led to the following conclusions about the impingement phenomena:

1. A critical parameter K, as a function of Reynolds and Ohnesorge number of the impinging droplet, was found to identify the boundary between droplets which deposit and those which reatomise and is defined in Eq. (1). For a plane surface of similar nondimensional roughness to the smooth spheres used in this experiment, K is 90. For a sphere of diameter 800 μm, K decreases to 49.
2. For impinging K above the critical value, reatomisation from the crown produced by an impinging droplet will occur through the merger of the rim on either side of cusps growing upon the crown, producing finger-like structures which subsequently disrupt into reatomised droplets. The effect of increased surface curvature has been found to promote the onset of reatomisation since the crown diameter decreases with decreasing surface diameter, allowing rim merger at the cusps to occur for lower critical K.
3. By analysing the velocity history of the crown rim, the reatomised droplets were seen to leave the rim with a vertical velocity component in the same direction as, and with magnitude approximately 25% of U, the velocity of the impinging droplet. The radial velocity of the crown at the times at which the reatomised droplets were produced was around 40% of U.
4. The reatomisation process from impingement onto smooth spheres has been shown to exhibit a high level of repeatability, implying deterministic flow within the crown. It is believed that the initial disturbances that lead to cusp formation and influence the eventual breakup are governed by the surface morphology of the target sphere. This was supported by experiments with spheres with surface asperities of size 20 and 40 μm, which were seen to cause the crown to start to breakup around 20 μs earlier than for the smooth surface.

Acknowledgements

The authors wish to thank Mr. John Laker for his help with the design and construction of the electronic instrumentation and Mr. Paul Jobson for manufacturing the mechanical equipment that was needed for this study. Mr. Hector Pergamalis developed the technique for producing artificially roughened surfaces by coating the target spheres with glass beads.

References

Bowden, F.P., Field, J.E., 1964. The brittle fracture of solids by liquid impact, by solid impact, and by shock. Proc. Roy. Soc. Lond. A282, 331–352.

Cossali, G.E., Coghe, A., Marengo, M., 1997. The impact of a single drop on a wetted solid surface. Exp. In Fluids 22, 463–472.

Ghielmetti, C., Marengo, M., Steigleder, S., Tropea, C., 1997. Droplet impingement on a solid surface covered by a liquid film. In: Proc. 13th Ann. Conf. On liquid Atomisation and Spray System – ILASS Europe. 97, 465–472.

Levin, Z., Hobbs, P.V., 1971. Splashing of water drops on solid and wetted surfaces. Phil. Trans. R. Soc. Lond. Ser. A269, 555–585.

McCarthy, M.J., Molloy, N.A., 1974. Review of stability of liquid jets and the influence of nozzle design. Chem. Engrg. J. 7, 1–20.

Mundo, C., Sommerfield, M., Tropea, C., 1995. Droplet-wall collisions: experimental studies of the deformation and breakup process. Int. J. Multiphase Flow 21 (2), 151–173.

Stow, C.D., Hadfield, M.G., 1981. An experimental investigation of fluid flow resulting from the impact of a water drop with an unyielding dry surface. Proc. Roy. Soc. Lond A373, 419–441.

Yarin, A.L., Weiss, D.A., 1995. Impact of drops on solid surfaces: self-similar capillary waves, and splashing as a new type of kinematic discontinuity. J. Fluid Mech. 283, 141–173.